DOI: 10.17277/amt.2016.03.pp.061-068

A Study of Some Physical Problems of Water Condition and Mass Transfer in Cellulose Acetate and Dynamic Membranes

A.A. Lavrenchenko[a], D.S. Lazarev[a], I.V. Khorokhorina[a],
Yu.M. Golovin[b], P.M. Polikarpov[b], S.I. Lazarev[a]*

[a] *Department of Applied Geometry and Computer Graphics,*
[b] *Department of Physics, Tambov State Technical University,*
112, Michurinskaya St., Tambov, 392032, Russian Federation

* Corresponding author: Tel.: + 7 (4752) 630370. *E-mail:* geometry@mail.nnn.tstu.ru

Abstract

The paper presents experimental study of physical water condition and mass transfer in cellulose acetate and dynamic semipermeable membranes by infrared spectrometric and hydrodynamic methods. The authors found that OH-groups of cellulose acetate form a nonequilibrium grid of hydrogen bonds between molecules and their fragments in the amorphous phase of the semipermeable membrane in the air-dried sample. The water molecules adsorbed on active —OH and —C = O groups, particularly in the amorphous phase, create additional negative charge on the molecules of cellulose acetate resulting from the orientation of the water dipoles, which leads to electrostatic repulsion of broken, stranded molecule fragments and straightening of polymer molecule while breaking intermolecular hydrogen bonds. Thermogravimetric studies to find out the structural organization of hydrogen bonds and water condition in the samples of the semipermeable polymeric MGA-95 membrane showed that at temperatures in the air-dry and water-saturated samples the membrane degradation process starts and ends with mass loss and endothermic effect.

The research proves the fact of dynamic membranes formation on the ultrafilters from water starch solutions. Due to the changes in condition and volume of water in the dynamic layer of the membrane, it is possible to change kinetic coefficients, i.e. to regulate the process of baromembrane separation of industrial water solutions. Electro-kinetic characteristics of reverse osmosis semipermeable membranes were studied. The experimental curves of the potential depending on sorption of sodium bicarbonate by MGA-95 and LSA-100 membranes were obtained. The discrepancy between the calculated and experimental data did not exceed 10 %. The method devised for determining the membrane potential in the process of sorption of sodium bicarbonate can be used as a testing methodology of polymeric semipermeable membranes.

Keywords

Dynamic layer; infrared spectrometric membrane method; intermolecular bonds; liquid crystal phase; membrane; potential; sorption; thermogravimetry.

Introduction

Membrane technology as a promising method comparing to other traditional methods is used for industrial wastewater and water solutions treatment, but the problem of water condition used in the semipermeable membranes remains controversial [1 – 3]. The role of bound and capillary water in membrane is based on the fact that a membrane has crystalline and amorphous regions, wherein the crystalline regions do not have obvious influence on the water and solute transfer. Water molecules, penetrating into the amorphous regions, are linked with the polymer functional groups by hydrogen bonds. The resulting layer of bound water has an ordered structure and has no solubility. The formation of strong hydrogen bonds with the surface ions of pores in the amorphous regions and crystallite membrane defects leads to the rupture of the supramolecular structure of the polymer membrane, to a greater or lesser extent.

The objective is to study some physical problems of the water condition in cellulose acetate and dynamic membranes by infrared spectrometric and hydrodynamic methods.

Experimental

The experimental study of the physical water condition in an acetate cellulose membrane determined IR spectra of the diffuse reflection from the surface

of the polymer membrane. IR spectra were recorded on a FT/IR-6200FTIR spectrometer, Japan. Thermogravimetric properties were studied on the EXSTAR TG / DTA 7200analyzer, Japan. TG, DTG, and DTA curves were recorded at a rate of 5 °C /min in the range from 16 to 200 °C. The experiment was conducted on two samples of the membrane (MGA-95), one of which was stored in a closed container with dry air environment, and the other was put into the water environment for 3 hours for the process of its saturation with water at room temperature. Cellulose acetate membrane samples of MGA-95 series were porous polymer cellulose acetate films (semitransparent color) on the nonwoven polyester and polypropylene substrates.

The formation of the dynamic membranes was studied using wastewater solutions in the alcohol-yeast production of Tambov biochemical companies in the process of ultrafiltration separation. The obtained solution was passed through the membrane device fitted with a separation flat-chambered cell using ultrafiltration membranes (UAM-150 cellulose acetate and UPM-K polysulfone amide). The study was conducted during the cold season. When the membrane pre-washing from the sorption impurities was finished, the separation cell was collected and inserted into the device. Having checked the tightness of the units, the device was set into the operation mode and left with the solution for 10–18 hours. Then, a test experiment was performed in order to identify the constant performance with retention membranes coefficient. Next, a series of basic experiments were carried out, during which the samples of the feed solution and permeate were taken; the permeate flow volume, pressure, and temperature were measured, and the flow rate of feed solution was monitored. The analysis of solutes in the water mass was performed by dichromate oxidizability. The retention coefficient was calculated by the following formula:

$$R = 1 - \frac{C_p}{C_0}, \qquad (1)$$

where R is retention coefficient; C_p is solute concentration in the permeate, kg/m^3; C_0 is solute concentration in the feed solution, kg/m^3.

Results and Discussion

To identify the process of water sorption, the potential differences across MGA-95, MGA-100 membranes were studied. The measurements were performed by the methods described in [4] in a demountable cell (Fig. 1) with two symmetrical vessels, in which carbon electrodes and manometric tubes were fastened. Membranes with an area

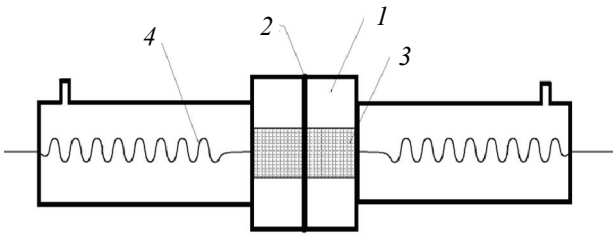

Fig. 1. The measuring cell:
1 – a threaded connection; *2* – a membrane;
3 – a carbon electrode; *4* – springs

of 78.5 mm^2 were fixed between the vessels using threaded connection. Electrodes with an area of 3.14 mm^2 were arranged coaxially at the surface of the membrane with a constant distance. The electrodes were made of the spectral carbon material impregnated with molten paraffin with subsequent polishing the ends. The vessels were filled with distilled water simultaneously.

The potential difference was measured by a INSTEKGDM-8246 high-resistance digital voltmeter, followed by the transmission of data through a COM-port to the PC with the ability to record in 0.5 s, which allowed us to monitor the value of the membrane potential $\varphi(t)$ in real time (Fig. 2).

To study the sorption of sodium bicarbonate, the potential differences across MGA-95, MGA-100 semipermeable membranes were measured in a demountable cell with two symmetrical vessels, in which carbon electrodes and manometric tube were fixed [5]. The semipermeable membranes with an area of 78.5 mm^2 were fixed between the vessels using threaded connection. The working area of electrodes was 3.14 mm^2. For experimental purposes the electrodes were made of spectral carbon material which was impregnated with molten paraffin with subsequent polishing the ends. The electrodes were coaxially arranged at the membrane surface at a constant distance. The vessels were filled with distilled water simultaneously.

The potential difference was measured by a INSTEKGDM-8246 high-resistance digital voltmeter, followed by the transmission of data through a COM-port according to a specially created program of data collection in software components of a PC with the ability to record them in 0.5 s. This allowed us to monitor the value of the membrane potential $\varphi(t)$ in real time of making the experiment.

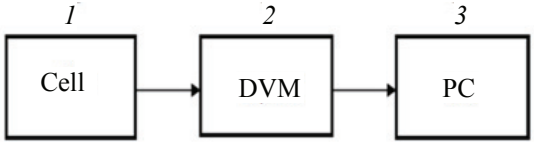

Fig. 2. Diagram of the setup to study membrane potential:
1 – a measuring cell; *2* – a digital voltmeter;
3 – a personal computer

The analysis of the experimental data according to the IR spectra of the air-dried and water-saturated samples (Fig. 3, curves *a* and *b*) in the frequency range from 600–1800 cm^{-1} oscillations of pyranose cycles and acetyl groups indicated their identity. This identical character excludes the possibility of different spatial arrangements of rotamers and pyranose cycles in the macromolecules of cellulose acetate.

However, significant differences between IR spectra in the frequency range of the methyl group valence vibrations CH_3 – 2852, 2920, 2985 cm^{-1} and hydroxyl OH-groups from 3000–4000 cm^{-1} (Fig. 3, *a*, *b*) can be noted. In the IR spectrum of the air-dried sample a broad, asymmetric intense absorption band with a maximum at 3290 cm^{-1} (Fig. 3, *a*) has been recorded. At the same time, we note that the low-frequency part of the band, relative to the maximum, has a slightly smaller area than high-frequency part.

At the same time, in the water-saturated sample (Fig. 3, *b*) the absorption band in the area from 3000–4000 cm^{-1} with a maximum of 3300 cm^{-1} has significantly less intensity, and its contour has protrusions at frequencies 3010, 3070, 3450, 3645 cm^{-1}. This fact deserves a special discussion. According to the concept of authors [4–6], the diffuse absorption band of stretching vibrations of OH groups indicates the formation of intra- and intermolecular hydrogen bonds with different length and energy. Fluctuations of the free hydroxyl groups are usually [5–7] recorded over 3650 cm^{-1}.

It is known that the water adsorption occurs primarily in the amorphous areas and partly on the surfaces of the crystallites. We should note that the amorphous phase is formed at a certain stage of the manufacturing cycle of cellulose acetate composite membrane production. It is a relatively symmetrical tangle of "broken", tangled and twisted macromolecules connected by the net of hydrogen bonds with different strengths. Therefore, in the IR spectrum of the air-dried sample it is observed structureless broad absorption band of OH groups in the 3000–4000 cm^{-1}. During swelling of cellulose acetate composite membrane sample water molecules are adsorbed on the hydrophilic active OH groups and carbonyl C = 0 hydrophobic acetyl groups to form proton-type hydrogen bonds. These hydrogen bonds are shown in projections at 3010–3070 cm^{-1} (Fig. 3, *b*), indicating the formation of cellulose acetate molecules with excess negative charge on atoms. The electric field, interacting with closely spaced negative atoms, pushes fragments of curved molecules and breaks the weak intermolecular hydrogen bonds. This leads to the

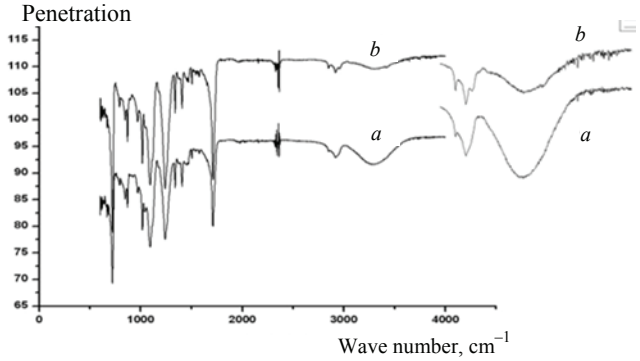

Fig. 3. IR spectra of the diffuse reflection from the surface of the MGA-95 cellulose acetate polymer membrane:
a – air-dried sample; *b* – saturated water sample

decrease in the intensity of the stretching vibrations of OH groups according to [6].

Thus macromolecules straighten and get the most stable form, which is formed around a layer of hydrated water molecules. Obviously, the layer structure is composed of water dipoles oriented perpendicularly to the axis of the polymer molecules, the negative pole of which is disposed in the outer side. As for the projection at 3450 cm^{-1}, its presence is likely to be connected with the interaction of water molecules of the first hydrated layer with associative water molecules of the next, the so-called destructive layer [5, 8]. Consequently, in the swollen sample of membrane the amorphous phase has a definite level of structural organization. One can safely assume that between coplanarly disposed cellulose acetate molecules there is a capillary space, which has likely a plane form and in which the water, acting as a plasticizer, pulls macromolecules together and keeps them in a stable state. Therefore, it is not surprising, that the X-ray diffraction studies [9] have shown changes in the distance between molecules from 1.13 to 1.03 nm. Thus, it should be noted that the water in these spaces is located in different associates: crystalline hydrate (frozen) absorbed (destructurized), in which the water molecules undergo approximately equal in magnitude but different in direction orienting influence of the neighboring water molecules and molecules of hydration shell. Destructurized water layer borders the diffuse layer in which the water retains normal properties [8] and shows the oscillations of OH groups with frequency 3645 cm^{-1}. Such ordering of associates of water on the surfaces of cellulose acetate molecules corresponds to the structure of the electric double layer, the zeta-potential of which is reduced in magnitude during the swelling of the MGA – 95 membrane sample from 53 to 20 mV [10]. Thus the water promotes the transition of the amorphous phase in the liquid-crystalline (**LC**) phase with anisotropic characteristic properties [11]. In our

studies, these properties are observed in the absorption splitting band of doubly degenerate antisymmetric stretching vibration of a methyl group with CH_3 for 2921 cm^{-1} air-dried sample into two bands with maxima at 2921 and 2985 cm^{-1} in the swollen sample (Fig. 3, *a*, *b*).

To clarify the structural organization of hydrogen bonds and water condition in the polymer membrane samples, both additional, thermogravimetric and DTA studies were carried out (Fig. 4). It was found (Fig. 4, *b*), that at a temperature of 21 °C in a air-dry sample there starts a degradation process which ends at 50 °C with a 2 % weight loss (curve 2) and endothermic effect (curve 1). Subsequent temperature increase

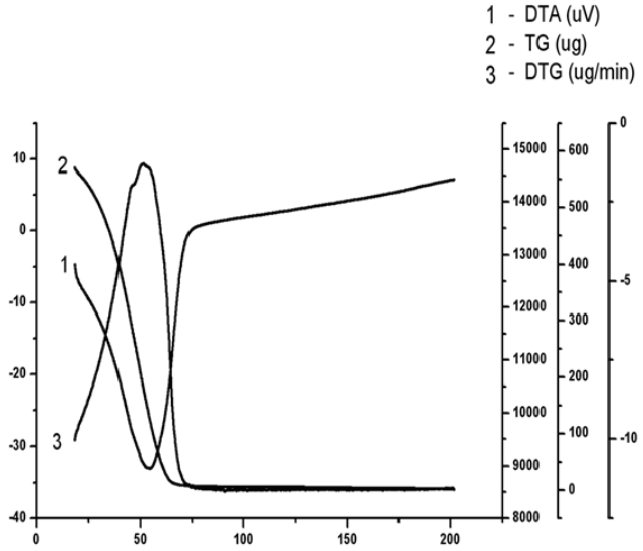

a)

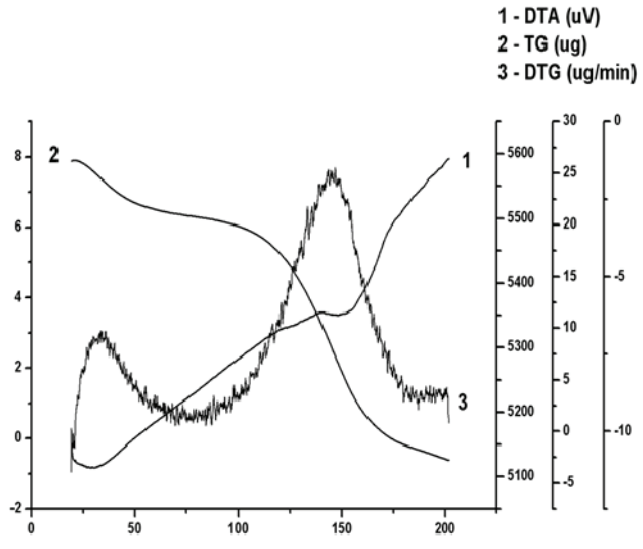

b)

Fig. 4. TGA dynamic curves of MGA-95 polymer membrane:
a – water-saturated sample; *b* – air-dry sample

results in the next endothermic effect (curve 1) from 120–175 °C with a maximum speed of weight loss (curve 3) at 146 °C, which ends at about 190 °C and amounts to 6.5 %.

Adsorbed moisture is likely to move away from the surface in this temperature range, but most importantly, the process of destruction of non-equilibrium hydrogen bonds occurs when water releases. An absolutely amazing picture is observed in the membrane sample saturated with water (Fig. 4, *a*). Mass loss (curve 2) starts at about 21 °C and ends at about 65 °C at a maximum speed (curve 3) at 51 °C and amounts to 42 % with a total moisture capacity of 70 % or more [12]. The process occurs with one endothermic effect (curve 1) from 20–65 °C. Note that easily removable water molecules at low temperatures are the water condensed on the membrane surface and pores without forming hydrogen bonds. They appear in the IR-spectrum in the form of protrusions of 3750, 3857 cm^{-1}. However, 28 % of the remained water is involved in the formation of structured LC phase to form a hydrate membrane, the destruction of which must occur at temperatures higher than 200 °C.

The experimental dependence of the retention coefficient of ultrafiltration membranes on the solutes concentration and operating pressure in water solutions of biochemical industries are shown in Fig. 5 and 6.

The kinetic curves in Fig. 5 and 6 showed that the retention coefficient increases with the increase in the operating pressure. The increase in the retention coefficient is caused by the decrease in water saturation in the dynamic membrane layer, the decrease in pore radius therein is caused by the adsorption interaction of solutes and substrate material (ultrafiltration membranes), which imposes additional steric limitations on the dissolved substances mass transfer. The increase of the solute concentration leads to the increases of the retention coefficient for the Fig. 4. TGA curves dynamic polymer membrane

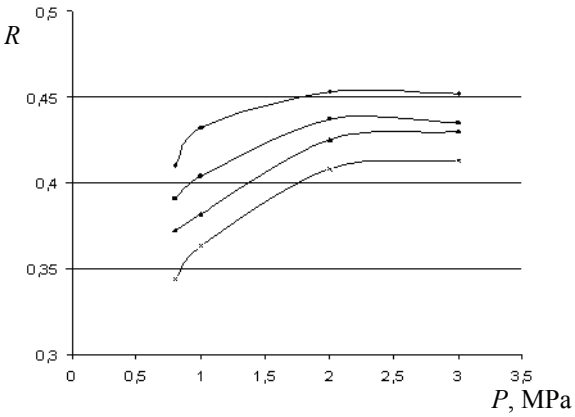

Fig. 5. The dependence of UAM-150 membranes retention coefficient on the concentration of the feed solution and pressure; concentrations, kg/m^3 are designated:
C_1 – 4.27; C_2 – 5.32; C_3 – 6.24; C_4 – 8.40

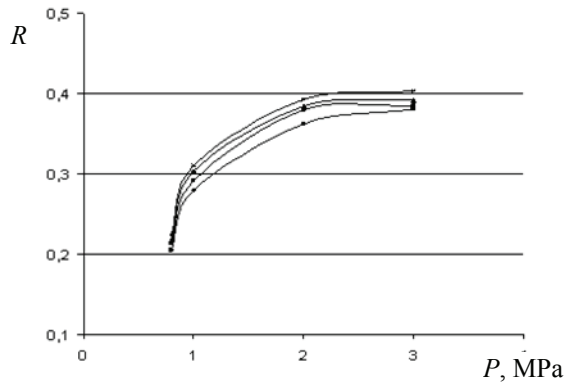

Fig. 6. The dependence of UAM-150 membranes retention coefficient on the concentration of the feed solution and pressure; concentrations, kg/m^3 are designated:
C_1 – 4.27; C_2 – 5.32; C_3 – 6.24; C_4 – 8.40

MGA-95: a water-saturated sample; b- air-dry sample.studied types of membranes (in the investigated range). This effect can be explained as follows: the solute sorbs membrane pore surface, and further increase of concentration leads to the volumetric filling of the membrane pores with the solutes and possibly blocking of the "smallest" pores. Furthermore, when the concentration is increased, the solution becomes "ordered", and it results in the formation of more complex spatial structures consisting of solute molecules, and possibly of water molecules both in the boundary layer and in the bulk solution, which also leads to the increase of membrane retention coefficient.

The retention coefficient also depends on the membrane type. In ultrafiltration membranes UAM-150 it is much higher than in the UPM-K membranes. This is due to the different nature of the solute interaction with the dynamic layer and the different pore structure of the active layer of the membranes [12–14].

The operating condition of the membrane is a swollen condition, therefore the study of transfer phenomena and kinetic parameters of the membrane was conducted in this state. The process of swelling of the semipermeable membrane with water results from the sorption processes affected by electric charges generated by the membrane potential difference, which, therefore, suggests some connection with the flow of ions, molecules of the solution in the pore space of the membrane [1, 15].

The experimental data on the dependence of the potential on the time of water sorption process of MGA-95 and MGA-100 type of reverse osmosis semipermeable membranes are shown in Fig. 7.

The analysis of the obtained data on water sorption (Fig. 7) made it necessary to measure the potential on the MGA-95, MGA-100 membranes

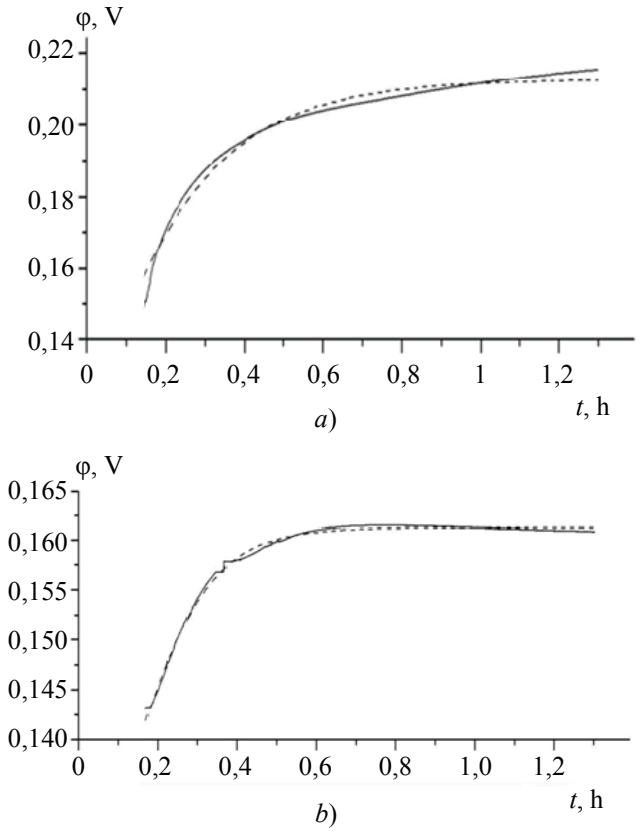

Fig. 7. Dependence of the potential on membrane water sorption:
a – for MGA-100 membranes; *b* – for MGA-95 membranes
(curves: — – experimental, ---- – theoretical)

in direct osmosis. In this case, the vessels were simultaneously filled with solvent (distilled water) at one side, and a 5 % solution of soda ($NaHCO_3$) at the other side.

The experimental curves under the simultaneous action of diffusion and osmosis processes are presented as dependences of membrane potential on the time $\varphi = f(t)$ in direct osmosis in Fig. 8.

The comparative analysis of the curves $\varphi(t)$ (Fig. 7 and 8) reveals the dependence of the potential on the structural properties of MGA-100 and MGA-95 semipermeable membranes. The potential for both membranes increases during the first moments, reaching a maximum value of $\varphi = 160$ mV for a MGA-95 membrane and $\varphi = 260$ mV for a MGA-100 membrane. Then it decreases asymptotically and reaches $\varphi = 28$ mV for a MGA-95 membrane and $\varphi = 202$ mV for a MGA-100 membrane during the time interval over 12 hours (Fig. 8, curves – solid line).

The analysis and systematization of the experimental results using the ORIGIN6 program showed that in the process of sorption and direct osmosis of structurally different membranes one can trace a specific pattern. Thus, the functional

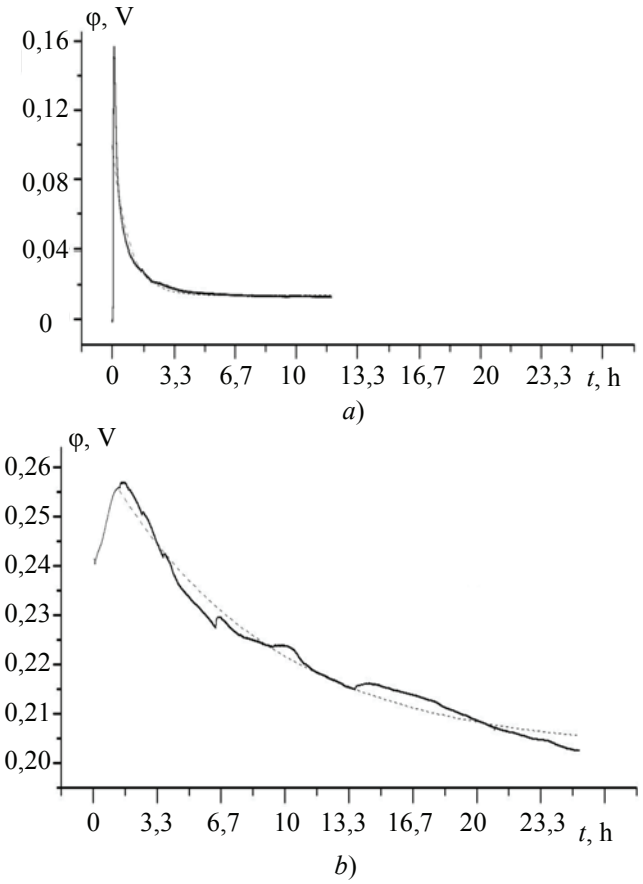

Fig. 8. Dependence of the membrane potentials on the time in full osmosis:
a – for MGA-100 membranes; *b* – for MGA-95 membranes (curves: — – experimental, ----- – theoretical)

dependence of the potential on time for water sorption can be represented by the equation:

$$\varphi = \varphi_{max} - \varphi_0 e^{-\beta t}, \quad (2)$$

where β is the coefficient of sorption and $\varphi_0 \cdot e^{-\beta t}$ – ζ-potential. Values φ_{max}, $\varphi_0 e^{-\beta t}$ = ζ-potential, β were calculated according to relaxation time and are presented in Table 1.

This equation describes well, on the one hand, the experimental curves in Fig. 7, and, on the other hand, the data on the sorption coefficient, and agrees with the values obtained in [15].

The function φ(*t*) for direct osmosis is an exponential dependence for an increasing part of the curve as equation 2 and a decreasing part as

$$\varphi_{osm} = \varphi_{min} + \varphi_0 e^{-P(t-\tau)}, \quad (3)$$

where *P* – is the coefficient of permeability (or relaxation); τ – membrane sorption time in the solution (for a MGA-95 membrane – 0.5*h*, for a MGA-100 membrane – 1*h*) up to a maximum potential.

Data β_1, *P*, $\varphi_0 e^{-P(t-\tau)}$ – ζ-potential are shown in Table 1.

Such a dependence suggests most probably that in the active membranes in the process of sorption there occurs a potential jump (Eq. 2) (ζ-potential), which contributes to its own membrane potential. Then, in the course of direct osmosis a decrease in potential takes place due to the changes in the direction of molecules and ions motion through the pores of the membrane by the value of the electrokinetic ζ-potential, and membrane potential tends to limit minimum values φ_{min} = 28 mV for MGA-95 and φ_{min} = 202 mV for MGA-100, but does not reach them (see Fig. 8).

Thus, we can assume that at a certain time (t_p) there comes a dynamic balance between the hydrodynamic force, determined by osmotic pressure ($\pi = \rho g h$) and the electromotive force of the membrane potential. This moment, of course, is associated with the relaxation time (permeability coefficient *P*) as $t_p \geq (1/P)$. At the same time ζ-potential changes its sign from the negative value for sorption to the positive one for osmosis. The calculated values of coefficients of sorption, permeability and the ζ-potential of MGA-95 the MGA-100 semi-permeable membranes correlate with the coefficients given in [16] and are shown in Table 2.

Thus, we can assume that at a certain time (t_p) comes a dynamic balance between the hydrodynamic force, determined by osmotic pressure ($\pi = \rho g h$) and the electromotive force of the membrane potential. This point, of course, associated with the relaxation time (permeability coefficient *P*) as the $t_p \geq (1/R)$. Thus ζ-potential changes sign from negative values for sorption to positive at osmosis. The calculated values of sorption, diffusion and the ζ-potential semi-permeable membranes MGA-95 and LSA-100 correlated with the factors given in [16] and are shown in Table 2.

Table 1

Data on ζ-potential in sorption and reverse osmosis

Membrane brand	Sorption				Direct osmosis				
	ζ-potential		φ_{max}, mV	β, $\times 10^{-3}$, s^{-1}	ζ-potential		φ_{min}, mV	β_1, $\times 10^{-3}$, s^{-1}	P_x, $\times 10^{-5}$, s^{-1}
	min, mV	max, mV			min, mV	max, mV			
MGA-95	–19.6	–53	164	9	+26	+70	28	5.5	11
MGA-100	–27	–75	215	5	+23	+62	202	2.5	3.4

Table 2

The experimental values of membrane potential depending of time

№	*t*, s	φ, V	№	*t*, s	φ, V
1	0.5	0.14382	44	22	0.14371
2	1	0.14352	45	22.5	0.14386
3	1.5	0.14328	46	23	0.14395
4	2	0.14320	47	23.5	0.14396
5	2.5	0.14299	48	24	0.14398
6	3	0.14295	49	24.5	0.14389
7	3.5	0.14273	50	25	0.14403
8	4	0.14269	51	25.5	0.14407
9	4.5	0.14276	52	26	0.14415
10	5	0.14272	53	26.5	0.14415
11	5.5	0.14259	54	27	0.14434
12	6	0.14263	55	27.5	0.14439
13	6.5	0.14301	56	28	0.14442
14	7	0.14296	57	28.5	0.14455
15	7.5	0.14308	58	29	0.14446
16	8	0.14307	59	29.5	0.14469
17	8.5	0.14320	60	30	014478
18	9	0.14320	61	30.5	0.14486
19	9.5	0.14318	62	31	0.14486
20	10	0.14322	63	31.5	0.14488
21	10.5	0.14318	64	32	0.14501
22	11	0.14319	65	32.5	0.14504
23	11.5	0.14317	66	33	0.14512
24	12	0.14314	67	33.5	0.14520
25	12.5	0.14309	68	34	0.14520
26	13	0.14311	69	34.5	0.14535
27	13.5	0.14313	70	35	0.14543
28	14	0.14314	71	35.5	0.14546
29	14.5	0.14313	72	36	0.14559
30	15	0.14313	73	36.5	0.14565
31	15.5	0.14313	74	37	0.14574
32	16	0.14314	75	37.5	0.14574
33	16.5	0.14314	76	38	0.14589
34	17	0.14314	77	38.5	0.14591
35	17.5	0.14314	78	39	0.14604
36	18	0.14314	79	39.5	0.14661
37	18.5	0.14314	80	40	0.14619
38	19	0.14323	81	40.5	0.14619
39	19.5	0.14333	82	41	0.14638
40	20	0.14331	83	41.5	0.14639
41	20.5	0.14333	84	42	0.14641
42	21	0.14342	85	42.5	0.14640
43	21.5	0.14346	86	43	0.14641
44	22	0.14354	87	43.5	0.14642

Conclusion

The experimental research on the water condition in cellulose acetate and dynamic membranes allows us to make the following conclusions:

1) the water molecules adsorbed on active –OH and –C = O groups, particularly in the amorphous phase, create additional negative charge on cellulose acetate molecules resulting from the orientation of the water dipoles, which leads to electrostatic repulsion of the "broken", stranded molecule fragments, straightening of polymer molecules while breaking intermolecular hydrogen bonds. It was found that water acting as a plasticizer, structures macromolecules of cellulose acetate membrane at the amorphous phase, making the transition to its LCD phase and forming additional capillary space;

2) the thermogravimetric studies aimed at finding out the structural organization of hydrogen bonds and water condition in the samples of the MGA-95 semipermeable polymeric membrane showed that at a temperature of 21 °C in a air-dry sample there starts a degradation process which ends at 50 °C with a 2 % weight loss (curve 2) and endothermic effect (curve 1). Subsequent temperature increase results in the next endothermic effect (curve 1) from 120 °C to 175 °C with a maximum speed of weight loss (curve 3) at 146 °C, which ends at about 190 °C and amounts to 6.5 %;

3) the process of baromembrane separation of industrial solutions for chemical plants allowed establishing the formation of dynamic membranes on ultrafilters from starchy substances in solution. Due to the changes in the structural characteristics of the dynamic membrane, i.e. by varying the technological parameters of the membrane process (in our case – the operating pressure), the separation baromembrane process for industrial water solutions may be controlled;

4) the study of electro-kinetic phenomena and their analysis and systematization allow us to believe that in the process of sorption and direct osmosis of structurally different membranes one can trace a specific pattern. This pattern is reflected in the fact that at a certain time there comes a dynamic equilibrium between the hydrodynamic force, determined by osmotic pressure and the electromotive force of the membrane potential. This is due to the

relaxation time, at the same time ζ-potential changes its sign from the negative value for sorption to the positive one for osmosis.

Acknowledgements

The work has been performed with the support of the state assignment in the sphere of scientific activity, task No. 2014/219 for 2014 – 2016.

References

1. Mulder M. (1999). Introduction to membrane technology: translation from English. M.: Mir, 513 p.

2. Ochkina K.A., Kulov N.N., Fomichev S.V. (1998). Theoretical foundations of chemical engineering, Vol. 32, no. 1, pp. 51-57.

3. Dubyaga V.P., Perepechkin L.P., Kovalevsky E.E. (1981). Polymer membrane, M.: Chemistry, 232 p.

4. Hydrogen bond. Ans. Edit. N.D. Sokolov, M.: Nauka, 1981, 285 p.

5. Zhbankov R.G., Kozlov P.V. (1983) Physics cellulose and its derivatives, Minsk: Science and Technology, 295 p.

6. Water in Polymers: Trans. from English, Ed. Roulenda. S., M.: Mir, 1984, 555 p.

7. Pankow S.P., Feinberg E.Z. (1976). The interaction of cellulose and cellulose materials with water, M.: Chemistry, 260 p.

8. Lazarev S.I., Golovin Y.M., Lazarev D.S. (2014). Membranes and membrane technology, Vol. 4, no. 3, pp. 208-211.

9. Golovin Y.M., Mitul I.P., Nikitenko D.A., Polikarpov V.M., Lazarev S.I., Horohorina I.V., Kholodilin V.N. (2014). Sorption and chromatographic processes, vol. 14, no. 3, pp. 530-536.

10. Shipovskaya A.B. (2009). *Fazovyiy analiz sistem efir tsellyulozyi-mezofazogennyiy rastvoritel*: Avtoref. … dis. d-ra him. nauk [Phase analysis of cellulose ether-mesophasegene solvent systems]. Saratov. (Rus)

11. Strathmann H. (2003). Membrane Science and Technology, vol. 9, Elsevier Science, 360 p.

12. Anil K. Pabby, Syed S.H. Rizvi, Ana Maria Sastre. (2008). Handbook of Membrane Separations: Chemical, Pharmaceutical, Food, and Biotechnological Applications. CRC, 316 p.

13. Enrico Drioli, A. Criscuoli, E. Curcio, (2005). Membrane Science and Technology vol. 11, Elsevier Science, 316 p.